

Apex jets from impacting drops

J. O. MARSTON¹ AND S. T. THORODDSEN²

¹A*STAR Institute of Chemical and Engineering Sciences, 1 Pesek Road,
Jurong Island, Singapore 627833

²Mechanical Engineering, National University of Singapore, 9 Engineering
Drive 1, Singapore 117576

(Received 28 June 2008 and in revised form 4 July 2008)

We present experiments showing vertical jetting from the apex of a viscous drop which impacts onto a pool of lower viscosity liquid. This jet is produced by the ejecta sheet which emerges from the free surface of the pool, and moves up and wraps around the surface of the drop. When this sheet of liquid converges and collides at the top apex of the drop it produces a thin upward jet at velocities of more than 10 times the drop impact velocity. This jetting occurs for a limited range of impact conditions, where the ejecta speed is sufficient for the sheet to travel around the entire drop periphery, but not so fast that it separates from the drop surface. The lower bound for the jetting region is thereby set by a minimal Reynolds number, but the upper bounds are subject to a maximum-Weber-number criterion. The strongest observed jets appear for viscous drops impacting onto liquid pools with the lowest viscosity as well as lowest surface tension, such as acetone and methanol. Jetting has also been observed for drops which are immiscible with the pool liquid, under a different range of impact conditions. However, jetting is never observed for pools of water, as the surface tension is then significantly larger than that of the drop. We believe that Marangoni stresses act in this case to promote separation of the sheet to prevent the jetting. A movie is available with the online version of the paper.

1. Introduction

The splashing during drop impact onto liquid and solid surfaces has received renewed research interest, Yarin (2006), due to improvements in imaging technology (Thoroddsen, Etoh & Takehara 2008) and the relevance to a wide variety of industrial processes, such as spray coating, cooling and cleaning of solid surfaces. The impact of drops or solid spheres onto liquid pools generates a horizontal ejecta sheet, which travels up the solid or separates to enter the air, as shown numerically by Weiss & Yarin (1999) and Josserand & Zaleski (2003) and experimentally by Thoroddsen (2002). Recent work by Duez *et al.* (2007) on the impact of a solid sphere highlights the importance of the wettability of the solid surface, showing that a superhydrophobic surface causes separation of the liquid sheet, to generate a large cavity, whereas a hydrophilic surface causes the sheet to hug the sphere surface. A similar observation was reported by Worthington & Cole (1900) using smooth vs. rough spheres and by May (1951) using spheres with clean vs. oil-contaminated surfaces.

Here we present experiments where a highly viscous drop replaces the solid sphere and impacts onto a low-viscosity, low-surface-tension pool. This liquid combination confines most of the deformations to the pool liquid and produces a thin horizontal ejecta sheet from the pool liquid, Thoroddsen (2002). For a limited range of impact

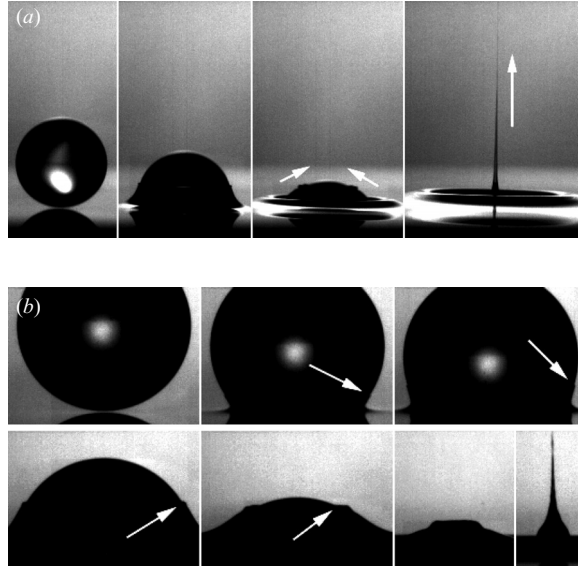


FIGURE 1. (a) The formation of the apex jets when a 90 % glycerin drop impacts onto a pool of 95 % ethanol/5 % methanol. The drop diameter $D = 4.1$ mm, $U = 2.1$ m s⁻¹ ($Re = 5700$, $We = 620$) and the frames are shown at $t = -0.04, 0.68, 1.32$ and 2.92 ms after first contact. See also the video available with the online version. (b) Close-up view for a pure glycerin drop impacting onto pure methanol. The arrows identify the methanol film travelling up the drop, for $D = 4.1$ mm and $U = 1.8$ m s⁻¹. Frames are shown at $t = -0.03, 0.23, 0.37, 0.97, 1.5, 1.98$ and 2.3 ms.

velocities this ejecta sheet stays attached to the drop, travelling up its sides and colliding at its apex, generating a fine high-speed vertical jet. Figure 1(a) and the supplementary video show this overall phenomenon and figure 1(b) shows a close-up of the drop surface, pointing out the tip of the methanol sheet. Note that these jets are qualitatively different from the well-known Worthington jets which are produced by the collapse of impact craters. In some of our cases, both the fine high-speed apex jet and a Worthington jet were observed; however, we focus on the former, new, jetting process.

2. Experimental setup

This phenomenon was observed in a limited range of the relevant parameters, i.e. the Reynolds, Weber and Marangoni numbers,

$$Re = \frac{\rho UD}{\mu}, \quad We = \frac{\rho DU^2}{\sigma}, \quad We_{\Delta\sigma} = \frac{\rho DU^2}{\Delta\sigma}, \quad M = \frac{\Delta\sigma \ell}{\rho\nu\alpha}$$

where D and U are the drop diameter and impact velocity; ρ , μ , ν and σ are the density, dynamic viscosity, kinematic viscosity and surface tension of the pool liquid; $\Delta\sigma = \sigma_d - \sigma_p$ is the surface tension difference between the drop and the pool and α is the diffusivity of the glycerin into the methanol ($\sim 10^{-9}$ m² s⁻¹). The characteristic length scale ℓ for the variable surface tension is here estimated by the thickness of the ejecta sheet, travelling up the drop.

The high- μ drop liquids were limited to high-concentration glycerin/water mixtures and silicone oils (*Shin-Etsu Chemical Co.*), whereas the pool liquids included ethanol,

Liquid	Density ρ [g cm ⁻³]	Viscosity μ [cP]	Surface tension σ [dyn cm ⁻¹]
Glycerin	1.26	~1000	65.0
Acetone	0.791	0.306	23.7
Methanol	0.793	0.593	22.5
Ethanol	0.789	1.19	23.2
Silicone oil 0.65 cSt	0.760	0.494	15.9
Silicone oil 1.00 cSt	0.818	0.818	16.9
Silicone oil 100 cSt	0.965	96.5	20.4
Silicone oil 350 cSt	0.970	340	21.1
Distilled water	0.996	1.004	72.1

TABLE 1. Properties of the different liquids used in the experiments.

methanol, acetone and various low-viscosity silicone oils. Some liquid properties are given in table 1. For our range of experiments a drop of $D \sim 4$ mm and impact velocities $1 \leq U \leq 2.5$ m s⁻¹ give values of We between 170 and 900, while Re takes values between 2000 and 25 000. These values show that the overall impact dynamics are inertia dominated. We will, however, show that the jetting is dependent on the dynamics of the thin ejecta sheet, which is significantly influenced both by viscous stresses and surface tension forces.

The large value of $M \sim 3 \times 10^6$ shows that molecular diffusivity cannot neutralize the Marangoni stresses due to $\Delta\sigma$, over the small time scales involved. The effects of these stresses are therefore better characterized by $We_{\Delta\sigma}$.

The large viscosity of the drop quickly dampens all oscillations following the pinch-off from the nozzle and the drop is therefore approximately spherical at impact. The fairly low release heights, less than 30 cm, typically cause less than 2% flattening of the drop shape by air resistance. The high viscosity of the drop also reduces its deformation as it penetrates the pool, with the downwards velocity of its top reduced only slightly by the added mass of the induced motions inside the pool. Note that even for significantly lower viscosity drops, e.g. 85% glycerin drop ($\mu = 140$ cP), the overall dynamics are quantitatively similar. The same is true for drops of silicone oil with $\nu = 100$ and 350 cSt.

The apex jetting was observed with high-speed video cameras (Photron Fastcam Ultima APX and SA-1) at frame rates up to 40 000 f.p.s. This frame rate corresponds to an image resolution of at least 128×256 pixels.

3. Results

3.1. Overall ejecta motions

Figure 2 shows the trajectory of the tip of the sheet, relative to the pool, which was traced from the video frames. As the sheet converges at the top of the drop its tip is obscured by the thicker leading edge of the sheet but, as shown schematically in figure 2(c), we believe the contact line impacts first, generating the thin rapid jet. However, sometimes a curved front impacts above the contact line and a small bubble is entrained (see figure 2d), but the jetting is little affected. Figure 2(a) shows four trajectories for identical glycerin drops impacting, at the same velocity, onto different miscible pools. These liquids were chosen to vary the viscous and Marangoni stresses, i.e. pure methanol, (90% methanol/10% water); (95% ethanol/5% methanol) and

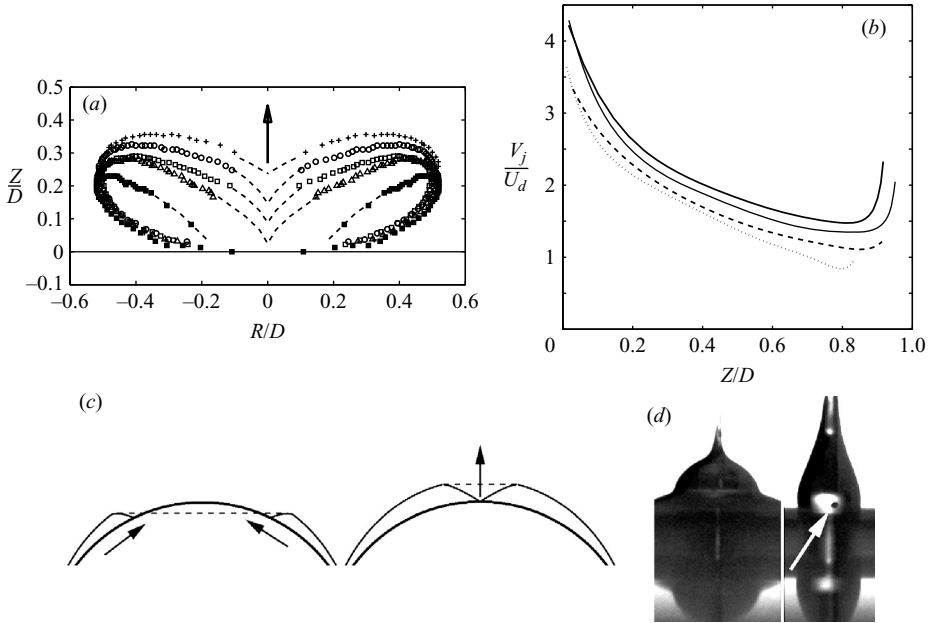


FIGURE 2. (a) Trajectory of the tip of the ejecta sheet as it travels up along the glycerin drop, normalized by drop diameter. For the bottom 4 curves $D = 4.1$ mm and $U = 1.86$ m s⁻¹, with different but miscible pool liquids: pure methanol (○); 90% methanol/10% water (□); 95% ethanol/5% methanol (△) and pure water (■). The top curve (+) shows the trajectory for the fastest moving sheet observed, i.e. when a drop of silicone oil (350 cSt) impacts onto an acetone pool ($D = 3.4$ mm, $U = 2.3$ m s⁻¹). The trajectories are taken from 30 kfps video sequences. The dashed curves indicate our estimate of the motions obscured during the convergence of the thick edge of the sheet. (b) Velocity of the tip of the enveloping film as a function of its height along the drop, for the conditions in (a), normalized by the impact velocity of the drop. Acetone (thick solid line), methanol (thin solid line), 95% ethanol (dashed line) and pure water (dotted line). The curves end where the contact line becomes obscured by the thicker jet. (c) Sketch of the convergence of the contact line. (d) Bubble entrapped inside the jet.

pure water. The ejecta sheet in water cannot reach the apex and no jetting is produced, while all the other combinations result in an apex jet. Of these four pool liquids the methanol sheet travels fastest up the drop thereby reaching farthest above the original pool surface and producing the strongest jetting. However, even faster sheets are observed for acetone impacted by a partially miscible drop of silicone oil, as is shown in the top curve. The apex jets emerge typically at velocities around 15 m s⁻¹ but as high as 25 m s⁻¹, i.e. at more than 13 times the impact velocity of the drop. Based on the resolution of the video we estimate that the initial diameter of the jet can reach less than 30 μm. Keep in mind that slight asymmetries often cause the jet to emerge at an angle, especially near the limits of the parameter range where jetting occurs.

3.2. Velocity of ejecta sheet

With the video data we can extract the velocity of the tip of the sheet V_j along the drop surface, as is shown in figure 2(b). The speed is measured relative to the drop surface and normalized by the impact velocity. It is clear that the contact line velocity is highest immediately after impact and then decelerates continuously along the drop surface, with only a slight acceleration as it converges close to the top. The sheets emerge at around 4 times the drop impact velocity in accordance with similar

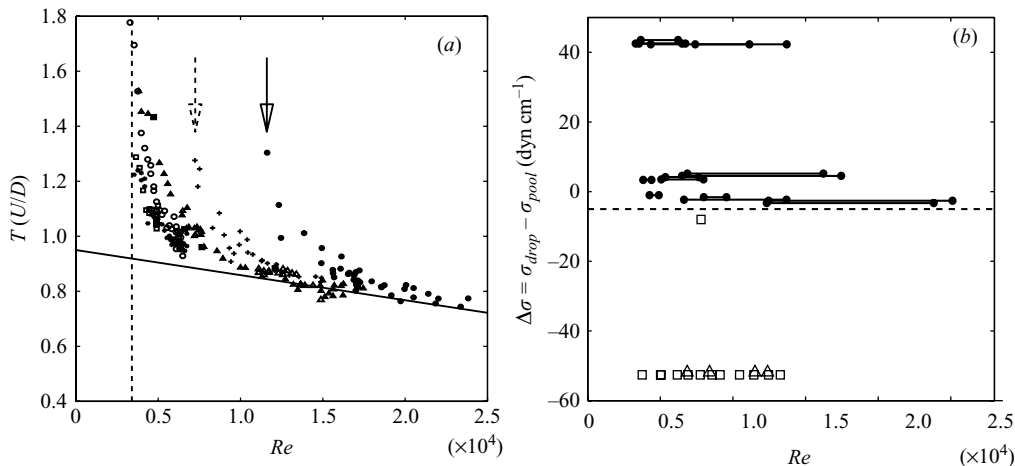


FIGURE 3. (a) The time T from first contact until start of the apex jetting vs. drop impact Re . Impact conditions: pool of 95 % ethanol/5 % methanol with a drop of: 100 % glycerin (\star), 90 % glycerin (\circ) and 85 % glycerin (\square); pure glycerin onto pure methanol (\triangle); methanol data for $U \simeq 1.8 \text{ m s}^{-1}$ over a range of drop sizes, $D = 1.7, 2.5, 3.0, 5.1 \text{ mm}$ (\blacksquare). Includes drops of silicone oil both 100 and 350 cSt onto lower viscosity silicone oils (0.65, 1.0 and 1.5 cSt) (\blacktriangle); methanol ($+$) and acetone (\bullet). (b) The parameter space where jetting is observed (solid lines between filled symbols) and not observed (open symbols).

experiments for homogenous liquids by Thoroddsen (2002). The curves cannot be extended to the apex, as the thicker edge blocks the location of the contact line, as is clear in figure 1.

These results show that the lowest viscosity pools, i.e. 0.65 cSt silicone oil, methanol and acetone, produce the most robust apex jets, owing to the ejecta sheet emerging from the pool at higher velocity as Re increases, as shown by Thoroddsen (2002). This is demonstrated in figure 3 which shows the travel time of the sheet T , measured from first contact of the drop with the pool until the appearance of the apex jet, for a range of impact Re . This time is normalized by the penetration time of the drop D/U . There exists a minimum Re where the film does not have enough momentum to reach the apex. Our estimate of this value is $Re_{min} \simeq 3400$. Secondly, the film velocity grows faster, with Re , than the impact velocity, as has been observed for separated ejecta sheets (Thoroddsen 2002). One can therefore expect stronger apex jets as Re increases.

Figure 3 also includes data for drops impacting on partly miscible and immiscible pools, i.e. silicone oils onto methanol and acetone. Both show Re_{min} which are larger than for miscible liquids, as indicated by the arrows in the figure.

3.3. Sheet separation

For higher impact velocities the ejecta sheet starts to develop azimuthal undulation and capillary instability breaks up the uniformity of the converging sheet, generating irregular or bent apex jets. We also observe twisted jets which may be rotating due to the convergence of azimuthally irregular contact lines. The boundary where the pronounced apex jet disappears is not very sharp, with irregular jetting setting in over an upper range of impact velocities. Significantly, the upper range of Re varies between the different pool liquids, with $Re_{max} \simeq 7000$ for 95 % ethanol, $Re_{max} \simeq 14000$ for methanol and $Re_{max} \simeq 24000$ for an acetone pool. The corresponding Weber numbers are considerably closer, considering the difference in miscibility, i.e. $We_{max} \simeq 700, 900$

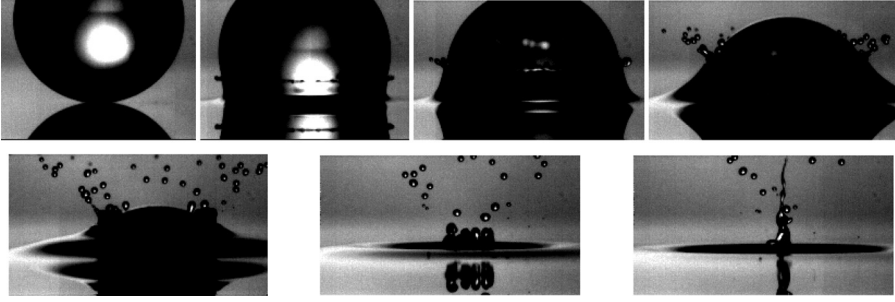


FIGURE 4. Separation of the sheet from the drop surface. The drop is pure glycerol and the pool liquid consists of 95 % ethanol/5 % methanol, for $D = 4.1$ mm, $U = 2.1$ m s⁻¹ and $Re \simeq 7000$.

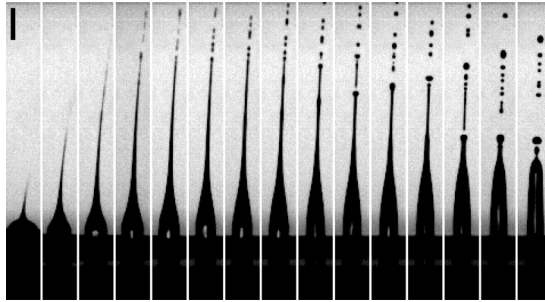


FIGURE 5. Breakup of the apex jet. The drop is pure glycerol and the pool liquid is methanol, for $D = 4.3$ mm, $U = 1.7$ m s⁻¹ and $Re \simeq 12000$. The scale bar is 1 mm and the frames are selected from a sequence spanning 4 ms.

and 1100 respectively. This indicates that surface tension plays a role in delaying the separation of the sheet from the drop surface. Furthermore, the difference in surface tension between drop and pool, $\Delta\sigma$, is important, as shown in figure 3(b) and discussed below.

For still higher impact velocities the sheet separates strongly from the drop surface, shedding liquid fingers and droplets. Figure 4 shows this separation for an impact onto a 95 % ethanol/5 % methanol pool. The detachment of the sheet is observed from the very start of the impact. This raises the question of whether the ambient gas plays a significant role in the separation process. Experiments at reduced pressure could resolve this issue, as with the present imaging system we cannot rule out the possibility of a microscopic air layer between the drop and the enveloping film. The detached sheet then exhibits a familiar fingering instability (much like the well-documented corona splash) with discrete droplets emanating from the tips (Xu, Zhang & Nagel 2005; Yarin 2006; Rioboo, Marengo & Tropea 2002). The irregular remnants of the contact sheet sometimes still collide at the top, generating irregular jetting.

3.4. Breakup of the jet

Figure 5 shows the breakup of the apex jet. Owing to its tapered shape, the jet starts breaking up first at the top, where it is thinnest. Subsequently it breaks into progressively longer segments, further down the jet. These segments contract, but also break up into numerous droplets. For the most robust jets, this breakup will typically produce 40 droplets, of sizes from 20 to 250 μ m in diameter. The nature of this

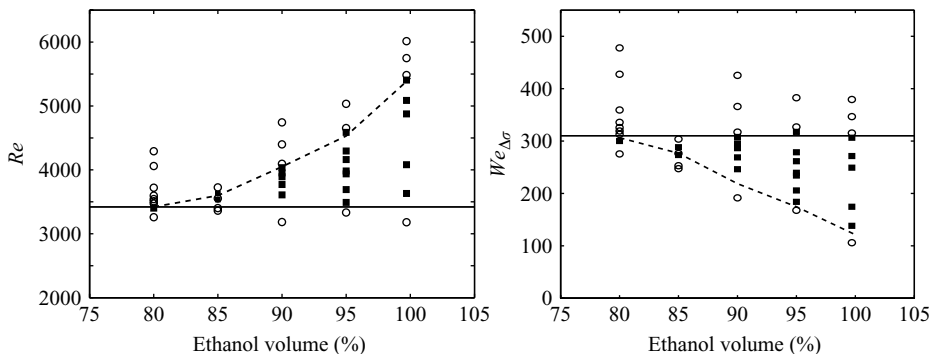


FIGURE 6. The parameter region where apex jetting occurs (filled squares) for a 90 % glycerin drop impacting onto ethanol/water mixtures of different volume fractions, shown both in terms of Re and $We_{\Delta\sigma}$.

breakup shows clearly that the jet consists purely of pool liquid, without the highly viscous drop liquid, which would produce elongated threads between the droplets.

4. Discussion

4.1. The role of surface tension and $\Delta\sigma$

The widely different value of Re_{max} observed in figure 3(a) for ethanol, methanol and acetone highlights the crucial role which surface tension plays in determining the upper bound for the jetting region. Figure 6 shows a set of experiments where we have used ethanol/water mixture to systematically vary the values of ν and σ . The drop ($D=4.0$ mm) is of 90 % glycerine/water mixture which is miscible with the pools. The data show clearly that the lower bound of the jetting region is set by a $Re_{min} \simeq 3400$ (see also figure 3a) and the upper limit corresponds to a constant $We_{\Delta\sigma} \simeq 320$ or $We \sim 550$. The values for these critical parameters will change for different liquid combinations, for example being sensitive to the miscibility and the sign of $\Delta\sigma$. However, detailed characterization of these effects is beyond the scope of the present work.

General conclusions can however be drawn about the significance of the Marangoni stresses generated by $\Delta\sigma$. This is clearly demonstrated in figures 2 and 3, where drop impacts, at similar Re , generated an apex jet for ethanol, but not for a water pool. Figure 7 compares the details of the ejecta sheets for two such cases. The water sheet, in panel (a), is much thicker than the methanol sheet in (b). Both liquid combinations are miscible, but have widely different $\Delta\sigma$ of -8 and 42 dyn cm^{-1} respectively. In other words, jetting does not occur when the pool has significantly higher surface tension than the drop. In all the experiments conducted herein, jetting is never seen for $\Delta\sigma < -6$ dyn cm^{-1} , see figure 3(b). However, this criterion is subject to further exploration of the relevant parameter space. It should be pointed out that the initial speed of Marangoni waves is of the same order of magnitude as the speed of the jet along the drop. This has for example been measured when a water drop comes in contact with an ethanol pool, by Thoroddsen *et al.* (2007b).

4.2. Effect of liquid miscibility

Figure 7(c–g) shows that this significance of $\Delta\sigma$ holds independently of the miscibility of the liquids, where we now use a drop of 350 cSt silicone oil impacting at the same velocity on different pools. Panel (c) shows the detailed shape and motion of the

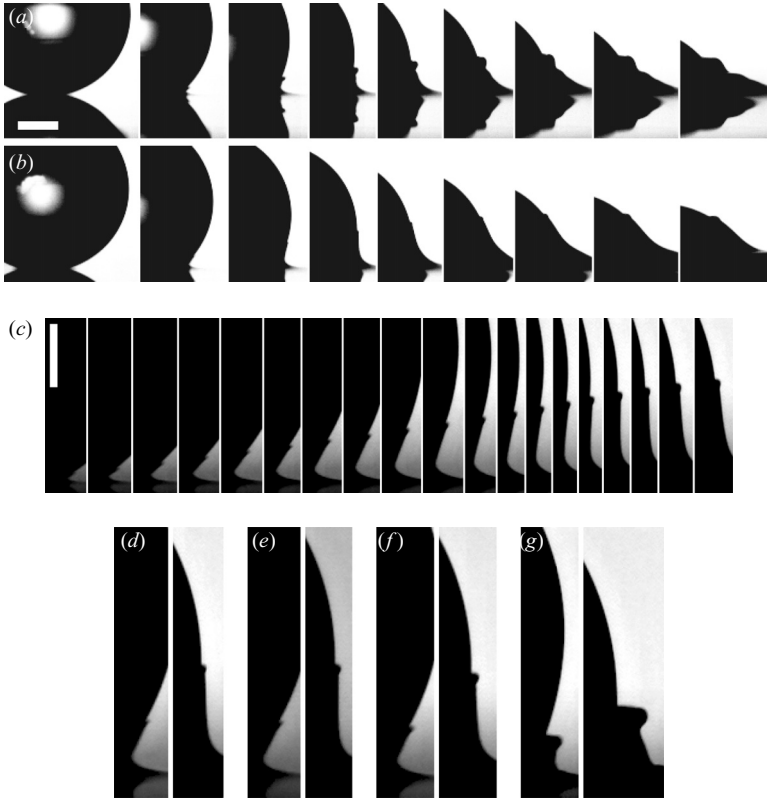


FIGURE 7. The pool sheet travelling up the drop during the impact of a glycerin drop onto water (*a*) and methanol (*b*), for $D = 4.1$ mm and $U = 1.86$ m s $^{-1}$. The panels are spaced by 5/30 ms. The scale bar is 1 mm. (*c*) Close-up of the sheet for a drop of silicone oil (350 cSt) onto an acetone pool ($Re = 15\,400$; $We = 350$). Panels spaced by 23 μ s, with first image 69 μ s after first contact. The scale bar is 0.5 mm. (*d*–*g*) The shape of the ejecta sheet for a drop of silicone oil ($\nu = 350$ cSt, $D = 3.4$ mm, $U = 1.94$ m s $^{-1}$) onto different pool liquids: (*d*) miscible silicone oil (0.65 cSt), $\Delta\sigma = \sigma_d - \sigma_p = 5.2$; (*e*) partly miscible acetone, $\Delta\sigma = -2.6$; (*f*) immiscible methanol $\Delta\sigma = -1.0$; (*g*) immiscible water $\Delta\sigma = -51.9$ mN m $^{-1}$.

sheet for partly miscible pool of acetone. Panels (*d*–*g*) then compare these shapes for miscible and immiscible pools, showing similar evolution, except for a water pool where $\Delta\sigma$ takes a large negative value and no jetting occurs. Note, that this is not due to the slightly lower Re for the water, as figure 8 clearly shows that the sheet always separates for a water pool over a wide range of Re and We .

4.3. Sheet dynamics

What mechanism causes the rapid deceleration of the ejecta sheet shown in figure 2(*b*)? Both viscous and surface tension forces will decelerate the tip of the sheet, as it travels up to the equator. The viscous boundary layer inside the sheet can be estimated from the travel time of the sheet. Typical travel time, as in figure 7, from first contact until the ejecta sheet reaches the equator, is about 0.5 ms, which gives a viscous length scale of $\delta \sim \sqrt{\nu T} \sim 20$ μ m inside a methanol sheet. This will cause significant deceleration, as the sheet thickness at the equator is of the order of 30–50 μ m. On the upper half of the drop the azimuthal component of the surface tension will assist in the closure

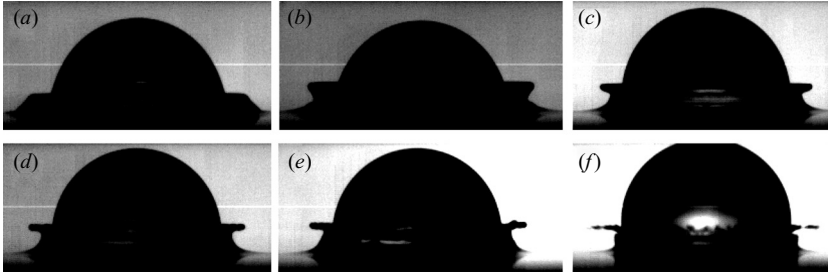


FIGURE 8. Sheet separation for silicone oil (100 cSt) impacting onto water, for a range of impact velocities; (a–f) $Re = 4200, 6000, 6500, 7200, 7800, 10\,400$; $We = 78, 155, 184, 224, 259, 463$.

of the film towards the apex, while the tangential component and the viscosity still act to decelerate the sheet.

Jetting in converging axisymmetric flow is often associated with inertial focusing, similar to the sheet meeting at the apex of our drop, see Renardy *et al.* (2003), Bartolo, Josserand & Bonn (2006), Thoroddsen, Etoh & Takehara (2007a) and the review by Eggers & Villermaux (2008). However, in the present flow configuration, there is a conceptual problem with inertial focusing in a thin layer of fluid. The pressure pushing the interface towards the apex, must also drive motions perpendicular to the sheet. This is indeed noted, by the large thickening of the sheet as it approaches the apex of the drop, see figures 1 and 7. The edge of the sheet has grown to a thickness of $\sim 200\ \mu\text{m}$ when it reaches about 30° from the pole. This thickening will clearly reduce the intensity of the inertial focusing simply by volume conservation.

4.4. Comparison with impact of a solid sphere

The top jetting observed for solid sphere impacts by Duez *et al.* (2007) (their figure 3a) is only superficially related to the present apex jets. This becomes clear by comparing the critical impact conditions for the fully wetting case of a glass sphere, $D = 25.4\ \text{mm}$, which is shown in the inset of their figure 2. They relate the critical impact velocity U^* to the capillary–viscous velocity σ/μ by

$$U^* \simeq 0.1 \sigma/\mu.$$

For our methanol pool this would give $U^* \simeq 3.8\ \text{m s}^{-1}$, with the corresponding critical $Re \simeq 1.3 \times 10^5$, an order of magnitude larger than the critical values for apex jetting, observed herein for the impacting viscous drop. However, Duez *et al.* focus on whether a large cavity is generated by the sphere impact and not whether a jet is formed.

The irregular jet shown in figure 4 produced by the collision of the separated sheet is indeed similar to the irregular jet observed in the solid case by May (1951) and Duez *et al.* (2007) where, even in the hydrophilic case, a multitude of fine tendrils of fluid have separated from the solid surface long before the contact line reaches the apex (their figure 3a). We also point out that both miscible and immiscible liquid combinations can generate apex jetting whereas the jetting in Duez *et al.* (2007) was limited to strongly hydrophilic conditions in the solid sphere case. Furthermore, it is well known (Thoroddsen *et al.* 2004) that in the early stages of the impact of a solid sphere on a liquid pool, a horizontal ejecta sheet is generated which separates from the surface of the sphere. In other words, whether a large cavity is generated by the impact of the solid sphere is unrelated to whether an ejecta sheet separates from the sphere following the initial contact with the pool. The cavity appears to be related to

contact line dynamics further up the sphere, whereas for the fine apex jets presented herein the ejecta sheets must remain attached to the drop.

5. Conclusions

We conclude that the observed apex jetting is confined by two competing effects. First, the low viscosity of the pool liquid, allows the generation of a thin ejecta sheet, which is fast enough to travel up to the apex before viscous forces and surface tension arrest its motion, thus implying a minimum Reynolds number for jetting which we estimate to be approximately 3400 for miscible liquids. Secondly, the inertia must not be too large, to avoid separation of the sheet from the drop surface. This upper bound is characterized by a Weber number criterion.

In addition, the surface tension difference, $\Delta\sigma$, can enhance attachment of the contact line, whereas liquid miscibility appears to be a much weaker influence in this new apex jetting phenomenon.

We thank Professor Victor Shim and the Impact Mechanics Laboratory at NUS for use of the high-speed video camera. We thank F. H. Zhang for help with some of the experiments.

REFERENCES

- BARTOLO, D., JOSSEMAND, C. & BONN, D. 2006 *Phys. Rev. Lett.* **96**, 124501.
 DUEZ, C., YBERT, C., CLANET, C. & BOCQUET, L. 2007 *Nat. Phys.* **3**, 180–183.
 EGGERS, J. 2001 *Phys. Rev. Lett.* **86**, 4290.
 EGGERS, J. & VILLERMAUX, E. 2008 *Rep. Prog. Phys.* **71**, 036001.
 JOSSEMAND, C. & ZALESKI, S. 2003 *Phys. Fluids* **15**, 1650–1657.
 MAY, A. 1951 *J. Appl. Phys.* **22**, 1219–1222.
 RENARDY, Y., POPINET, S., DUCHEMIN, L. *et al.* 2003 *J. Fluid Mech.* **484**, 69–83.
 RIOBOO, R., MARENGO, M. & TROPEA, C. 2002 *Exps. Fluids* **33**, 112–124.
 THORODDSEN, S. T. 2002 *J. Fluid Mech.* **451**, 373–381.
 THORODDSEN, S. T., ETOH, T. G. & TAKEHARA, K. 2007a, *Phys. Fluids* **19**, 052101.
 THORODDSEN, S. T., ETOH, T. G. & TAKEHARA, K., 2008 *Annu. Rev. Fluid Mech.* **40**, 257–285.
 THORODDSEN, S. T., ETOH, T. G., TAKEHARA, K. & TAKANO, Y. 2004 *J. Fluid Mech.* **499**, 139–148.
 THORODDSEN, S. T., QIAN, B., ETOH, T. G. & TAKEHARA, K. 2007b, *Phys. Fluids* **19**, 072110.
 WEISS, D. A. & YARIN, A. L. 1999 *J. Fluid Mech.* **385**, 229–254.
 WORTHINGTON, A. M. & COLE, R. S. 1900 *Phil. Trans. R. Soc. Lond. A* **194**, 175–199.
 XU, L., ZHANG, W. W. & NAGEL, S. R. 2005 *Phys. Rev. Lett.* **94**, 184505.
 YARIN, A. L. 2006 *Annu. Rev. Fluid Mech.* **38**, 159–192.